

Cover Page



Universiteit Leiden



The handle <http://hdl.handle.net/1887/22212> holds various files of this Leiden University dissertation.

Author: Wilde, Adriaan Hugo de

Title: Host factors in nidovirus replication

Issue Date: 2013-11-13

Chapter 2

The *in vitro* RNA synthesizing activity of the isolated arterivirus replication/transcription complex is dependent on a host factor

Martijn J. van Hemert, Adriaan H. de Wilde,
Alexander E. Gorbalenya, and Eric J. Snijder

J. Biol. Chem. (2008) vol. 283, no. 24, pp. 16525–16536

Reprinted with permission

ABSTRACT

The cytoplasmic replication of positive-stranded RNA viruses is associated with characteristic, virus-induced membrane structures that are derived from host cell organelles. We used the prototype arterivirus, equine arteritis virus (EAV), to gain insight into the structure and function of the replication/transcription complex (RTC) of nidoviruses. RTCs were isolated from EAV-infected cells and their activity was studied using a newly developed *in vitro* assay for viral RNA synthesis, which reproduced the synthesis of both viral genome and subgenomic mRNAs. A detailed characterization of this system and its reaction products is described. RTCs isolated from cytoplasmic extracts by differential centrifugation were inactive unless supplemented with a cytosolic host protein factor, which - according to subsequent size fractionation analysis - has a molecular mass in the range of 59-70 kDa. This host factor was found to be present in a wide variety of eukaryotes. Several EAV replicase subunits cosedimented with newly made viral RNA in a heavy membrane fraction that contained all RNA-dependent RNA polymerase activity. This fraction contained the characteristic double membrane vesicles (DMVs) that were previously implicated in EAV RNA synthesis and could be immunolabeled for EAV nonstructural proteins (nsps). Replicase subunits directly involved in viral RNA synthesis (nsp9 and nsp10) or DMV formation (nsp2 and nsp3) exclusively cosedimented with the active RTC. Subgenomic mRNAs appeared to be released from the complex, while newly made genomic RNA remained more tightly associated. Taken together, our data strongly support a link between DMVs and the RNA-synthesizing machinery of arteriviruses.

INTRODUCTION

Positive-strand RNA viruses form the largest group of animal viruses and include many important human pathogens, like poliovirus, hepatitis A and C virus, dengue virus, yellow fever virus, West Nile virus and various human coronaviruses. Although these viruses differ in many aspects of their biology, including genome size, organization, and expression strategy, they are united by the fact that their RNA genome is replicated by cytoplasmic enzyme complexes. These complexes are associated with virus-induced membrane structures that are derived from host cell organelles (for reviews see [75, 195, 196]). Such membrane structures might function as scaffold for the replication machinery, provide a suitable microenvironment for viral RNA synthesis, serve to recruit membrane-bound host proteins, and/or provide protection against the host cell's antiviral responses (e.g. RNA degradation or responses triggered by the double-stranded (ds) RNA intermediates of viral RNA synthesis).

Nidoviruses (corona-, roni-, and arteriviruses) have exceptionally large polycistronic RNA genomes and employ a unique transcription mechanism to produce a nested set of subgenomic (sg) mRNAs. Therefore, among positive-strand RNA viruses, nidovirus RNA synthesis is considered to be of unparalleled complexity [37, 196]. In nidovirus-infected cells, newly synthesized viral RNA and many replicase subunits were found to colocalize in discrete foci in the perinuclear region [32, 33, 35, 197-208]. Electron microscopy of this area revealed the presence of large numbers of typical paired membranes and double membrane vesicles (DMVs) [31, 32, 35, 201, 208-212]. For the coronaviruses mouse hepatitis virus (MHV) and SARS-coronavirus (SARS-CoV) and the arterivirus equine arteritis virus (EAV), immunoelectron microscopy revealed that both viral nonstructural proteins (nsps) presumed to be part of the replication/transcription complex (RTC) and de novo made viral RNA are associated with these membranes [31, 32, 35, 201]. Based on these results, DMVs have been postulated to carry the enzyme complex that is responsible for nidovirus replication and sg mRNA synthesis.

One of the best studied nidovirus models is the arterivirus prototype EAV, which has been used extensively to study both replicase functions and the mechanism of nidovirus RNA synthesis. Of the 12.7 kb EAV genome (RNA1) 75% is occupied by the large replicase gene that consists of the open reading frames (ORFs) 1a and 1b. The EAV replication cycle starts with the translation of RNA1 to synthesize two large replicase polyproteins: the 1727-aa ORF1a-encoded pp1a and the 3175-aa pp1ab, which is synthesized after a -1 ribosomal frameshift that occurs immediately upstream of the ORF1a termination codon and results in the extension of pp1a with the ORF1b-encoded part of the replicase (reviewed in [213]). Subsequently, pp1a and pp1ab undergo extensive autoproteolytic processing by three ORF1a-encoded proteases, which leads to the generation of 13 end products (nsps), named nsp1 to nsp12 (a recently described cleavage within nsp7 yields

nsp7 α and nsp7 β [214]). Most of these replicase subunits appear to become associated with intracellular membranes in the perinuclear region of the infected cell [33, 201, 202], where they are thought to assemble into RTCs. The ORF1b-encoded subunits contain the core enzymatic activities that are involved in viral RNA synthesis, like the RNA-dependent RNA polymerase (RdRp) and RNA helicase [215, 216], while ORF1a encodes, in addition to the three protease domains, several putative trans-membrane subunits. The latter appear to play a more 'structural' role by inducing DMV formation [217] and presumably anchoring the RTC to intracellular membranes [32].

In EAV-infected cells, the RTC mediates the synthesis of genomic RNA (RNA1) and a nested set of six sg mRNAs (RNA2 - RNA7). These transcripts are 3' co-terminal and also contain a common 211-nt 5'-leader sequence that is identical to the 5' end of RNA1. Each sg mRNA is thought to be produced from its own subgenome-length minus strand template. The latter are produced via a mechanism of discontinuous minus strand RNA synthesis during which sequences encoding sg RNA "leader" and "body" are joined (for recent reviews, see [40, 196]). The production of a set of sg transcripts is a characteristic feature of nidoviruses and serves to regulate the expression of the viral structural protein genes from the 3'-proximal part of the genome. Therefore, their synthesis is referred to as 'transcription', to distinguish it from the process of replication. Viral RNA synthesis involves partially and fully double-stranded intermediates, known as replicative intermediates (RI) and replicative forms (RF), which are thought to be associated with plus- and minus-strand RNA synthesis, respectively [218, 219].

The isolation of replication complexes and the development of *in vitro* RNA synthesis assays (IVRAs) have proven to be valuable tools for studying the mechanistic details of the replication of several viruses. However, robust *in vitro* systems supporting the synthesis of the full spectrum of viral RNAs produced in nidovirus-infected cells have not been described and therefore we set out to develop such a system for EAV. The purification of active, membrane-associated RTCs should enhance our insight into their structure and function, including the molecular details of nidovirus replication and transcription. We now describe the development, optimization, and characterization of such an *in vitro* system for EAV, in which both genome-sized and sg RNAs, mainly of positive polarity, were synthesized. The characterization of partially purified and enzymatically active RTCs revealed that several EAV nsps, including the nsp9-RdRp, cosedimented with endogenous and newly synthesized viral RNA in fractions that contained double membrane structures. Subgenomic mRNAs appeared to be released from the RTC-containing fraction, while a large proportion of newly synthesized genomic RNA remained associated with it. Remarkably, the isolated RTC was not active unless it was supplemented with a preparation containing a cytosolic host protein factor. This host factor was found to be present in a wide variety of eukaryotes, and its preliminary characterization indicated that it has a molecular mass in the range between 59 and 70 kDa.

MATERIALS AND METHODS

Cells, virus and antisera

BHK-21 cells were cultured and infected with EAV (Bucyrus strain) at a multiplicity of infection of 5, essentially as described [220], except that cells were grown in GMEM (Gibco) supplemented with 5% or 2% fetal calf serum before and after infection, respectively. HeLa cells and Vero E6 cells were grown in DMEM supplemented with 10% fetal calf serum. C6/36 cells were grown as described [221]. One-day old de yolked zebrafish embryos were obtained from Christoph Bagowski (Department of Integrative Zoology, Institute of Biology, Leiden University). *Saccharomyces cerevisiae* strain FY1679 was grown in YPD. A new nsp9 rabbit antiserum was raised against bacterially expressed recombinant nsp9 [215]. The other antisera used in this study have been described previously [201, 222, 223].

Isolation of enzymatically active RTCs from EAV-infected cells

Approximately 1×10^8 EAV-infected BHK-21 cells were harvested by trypsinization at 6 h post infection (p.i.), when infection was carried out at the commonly used temperature of 39.5°C, or 10 h p.i. when infection was done at 37°C. Cells were resuspended in 2 ml hypotonic buffer (20 mM HEPES, 10 mM KCl, 1.5 mM MgOAc, 1 mM DTT, 133 U/ml RNaseOUT (Invitrogen) and 2 µg/ml actinomycin D (ActD), pH 7.4). During harvesting and lysis 2 µg/ml ActD was present in all solutions used. The number of harvested cells was determined using a counting chamber and the percentage of infected cells was checked by immunofluorescence microscopy as described [33]. After incubation on ice in hypotonic buffer for 15 min, cells were disrupted in an ice-cold ball-bearing homogenizer (Isobiotek) with 16 µm clearance. HEPES, sucrose and DTT were added to yield a lysate containing 35 mM HEPES, pH 7.4, 250 mM sucrose, 8 mM KCl, 2.5 mM DTT, 1 mM MgOAc, 2 µg/ml ActD and 130 U/ml RNaseOUT. Nuclei, large debris and any remaining intact cells were then removed by two subsequent centrifugation steps at 1,000 x g and 4°C for 5 min and the post-nuclear supernatant (PNS) was either assayed immediately for RdRp activity or stored at -80°C, at which activity could be retained for at least 1 year. Protein concentrations were determined using the Bio-Rad protein assay reagent.

In vitro RNA synthesis assay (IVRA)

Following optimization of reaction conditions (as described under "Results"), standard 28-µl IVRA mixtures contained 25 µl of EAV-infected cell lysate (either PNS, S10, P10 or combinations), 30 mM HEPES pH 7.4, 220 mM sucrose, 7 mM KCl, 2.5 mM DTT, 2.5 mM MgOAc, 2 µg/ml ActD, 25 U RNaseOUT, 20 mM creatine phosphate (Sigma), 10 U/ml creatine phosphokinase (Sigma), 1 mM ATP, 0.25 mM GTP, 0.25 mM UTP, 0.6 µM CTP and 0.12 µM, 10 µCi [α -³²P]CTP (GE Healthcare). Unless otherwise indicated, standard reactions

were performed for 100 min at 30°C. Reactions were terminated by the addition of 60 µl 5% lithium dodecyl sulfate, 0.1 M Tris-HCl, 0.5 M LiCl, 10 mM EDTA, 5 mM DTT, 0.1 mg/ml Proteinase K, pH 8.0. After an incubation of 15 min at 42°C, unincorporated label was removed using RNase-free Micro Bio-spin 30 columns (Bio-Rad) and RNA was isolated, dissolved in 20 µl of 1 mM sodium citrate, pH 6.5, and analyzed as described below.

Isolation, gel electrophoresis and detection of RNA

RNA was isolated by acid phenol extraction and isopropanol precipitation with Glyco-Blue (Ambion) as coprecipitant, essentially as described [224]. Denaturing formaldehyde agarose gel electrophoresis was performed as described [225]. Semi-denaturing 7 M urea-3% polyacrylamide gel electrophoresis was performed essentially as described [226]. Before loading, samples were either incubated at 42°C for 15 min or heat-denatured for 3 min at 96°C, followed by rapid cooling on ice. For detection of IVRA products, PhosphorImager screens were directly exposed to dried gels, after which screens were scanned with a Personal Molecular Imager FX (Bio-Rad) and incorporation of label was quantified using Quantity One v4.5.1 software. Incorporation of [α - 32 P]CTP was quantified by correlating the measurements to those from membrane strips containing known quantities of [α - 32 P]CTP. For the detection of unlabeled EAV RNA, direct hybridization of agarose gels was performed [225] using a 32 P-labeled oligonucleotide probe (5'-TTG-GTTCCTGGGTGGCTAATAACTACTT-3') that is complementary to the 3'-end of all EAV mRNAs. For quantitative analysis, known quantities of *in vitro* transcripts were run on the same gel.

Hybridization of IVRA products

In vitro transcribed RNAs (1 µg) corresponding to the ORF7 region (nt 12313-12660) of the EAV genome (RNA7+) or its complementary sequence (RNA7-) were immobilized to Hybond N+ membrane (GE Healthcare). Equal amounts of total cellular RNA isolated from mouse L cells and full-length Sindbis virus RNA transcripts were included as negative controls. The membrane with the immobilized probes was hybridized (0.8 ml volume; 16 h at 60°C) with half of the 32 P-labeled RNA recovered from a 28-µl IVRA. Membranes were washed twice for 20 min at 60°C with 4 ml of 15 mM NaCl, 1 mM NaH₂PO₄, 0.1 mM EDTA, 0.05% SDS, pH 7.0. To confirm the specificity of the immobilized probes, membranes were also hybridized with either 32 P-labeled RNA7+ or 32 P-labeled RNA7- transcript. Hybridization was quantified by PhosphorImager analysis as described above.

LiCl fractionation and RNase treatment of IVRA products

IVRA reactions were terminated with lithium dodecyl sulfate and proteinase K as described above. After removal of unincorporated label, the LiCl concentration was raised to 2 M and samples were incubated at -20°C for 16 hours (40). RI and single-stranded

(ss) RNA were pelleted by centrifugation for 1 hour at 16,000 x g and 4°C. Pellets were washed with 70% ethanol, dried and dissolved in 1 mM sodium citrate. The 2 M LiCl supernatant was desalted using Micro Bio-spin 30 columns (Bio-Rad). Samples were treated with a mix of RNase A (2.5 U/ml) and RNase T1 (100 U/ml) under low salt conditions (15 mM NaCl, 2 mM sodium citrate pH 7.2) or high salt conditions (750 mM NaCl, 75 mM sodium citrate pH 7.2) for 15 min at 37°C. Double-stranded RNA was specifically degraded by incubation with RNase III (Ambion; 50 U/ml) for 15 min at 37°C in 650 mM NaCl, 60 mM sodium citrate, 10 mM MgOAc, 1 mM DTT, 10 mM Tris-HCl, pH 7.2. After RNase treatment, RNA was isolated as described above, except that the phenol extraction step was omitted.

Subcellular fractionation by differential centrifugation, ultrafiltration, and size exclusion chromatography

PNS fractions of BHK-21, HeLa, Vero E6, and C6/36 cells were prepared by mechanical disruption as described above for EAV-infected BHK-21 cells. A yeast PNS and a zebrafish PNS were prepared in a similar way except that yeast cells from a 50-ml culture were disrupted by vortexing in the presence of 500 µm diameter glass beads in 0.5 ml hypotonic buffer, and zebrafish cells from 200 one-day old zebrafish embryos were disrupted in 200 µl hypotonic buffer by passing them through a 27-gauge needle. The total protein concentration in all lysates was between 1 and 5 mg/ml. PNS fractions were centrifuged for 10 min at 4°C at 5,000 x g, 10,000 x g and 16,000 x g yielding supernatants S5, S10, S16 and pellets P5, P10, and P16 respectively. Pellets were resuspended in dilution buffer (35 mM HEPES, 250 mM sucrose, 8 mM KCl, 2.5 mM DTT, 1 mM MgOAc pH 7.4) by carefully pipetting (20x) in 1/5 to 1/10 of the volume of the PNS from which the pellet was prepared. For IVRAs, 5 µl of a pellet fraction was mixed with either 20 µl dilution buffer or 20 µl of a 'supernatant fraction', after which reactions were performed as described above. The S16 fraction was centrifuged for 1 h at 200,000 x g to yield a S200 supernatant fraction. Low molecular weight compounds (<6 kDa) were removed from S16 by size exclusion chromatography using Micro Bio-spin 6 columns (Bio-Rad), yielding fraction F>6. Ultrafiltration of S16 through filters with cut-off sizes of 10 kDa (Millipore Biomax 10K NMWL), 100 kDa (Millipore Biomax 100K NMWL) and 1000 kDa (Vivascience Vivaspin 1,000,000 MWCO) yielded filtrates F<10, F<100 and F<1000, respectively.

Gel filtration chromatography

A HeLa S200 fraction (240 µg protein in 200 µl) was fractionated by gel filtration chromatography using an ÄKTA FPLC (GE Healthcare) and a Superdex 200 HR10/30 column (GE Healthcare) at 4°C. The column was equilibrated with 20 mM HEPES, pH 7.4, 150 mM KCl, 2 mM DTT, 1 mM MgOAc. Elution was done in the same buffer, at a flow rate of 0.5 ml/min, and 0.5-ml fractions were collected after the first 7 ml (which represented the

void volume of the column). For each fraction, the buffer was exchanged to dilution buffer using Micro Bio-spin 6 desalting columns (Bio-Rad). The Superdex column was calibrated with the HMW calibration kit (GE Healthcare) to obtain size estimates for the protein fractions obtained.

Protease and nuclease treatment

Fraction S16 was treated for 15 min at 30°C with 2 mg/ml, 0.4 mg/ml, 0.08 mg/ml and 0 mg/ml of proteinase K, after which the protease was inactivated by adding 2 mM PMSF and samples were cleaned up with Micro Bio-spin 6 columns (Bio-Rad). Inactivation of proteinase K by this procedure was confirmed by testing the stability of ³⁵S-labeled control proteins during a 100-min incubation. S16 was treated with 75 U/ml of micrococcal nuclease (Fermentas) in the presence of 2 mM CaCl₂ for 30 min at 30°C, after which the nuclease was inactivated by the addition of 5 mM EGTA. The extent of RNA degradation was monitored using a ³H-uridine-labeled *in vitro* transcript.

SDS-PAGE and Western blot analysis

After SDS-PAGE, proteins were transferred to Hybond-P PVDF membrane (GE Healthcare) by semi-dry blotting. Membranes were blocked with 1% casein in PBS containing 0.1% Tween-20 (PBST) and were incubated with mono-specific anti-EAV replicase rabbit antisera: anti-nsp1 (1:2000), anti-nsp2 (1:2000), anti-nsp3 (1:2000), anti-nsp4 (1:2000), anti-nsp7-8 (1:2000), anti-nsp9 (1:5000) or anti-nsp10 (1:2000) antisera, all diluted in PBST containing 0.5% casein and 0.1% BSA. Peroxidase-conjugated swine anti rabbit IgG antibody (DAKO) and the ECL-plus kit (GE Healthcare) were used for detection. The SilverQuest kit (Invitrogen) was used for silver staining of SDS-PAGE gels.

Electron microscopy

Formvar-coated grids were placed on top of 25- μ l drops of P10 fractions and incubated at room temperature for 1 minute. After blocking with 1% BSA in PBS, grids were incubated with a rabbit anti-nsp3 or preimmune serum (1:200) in PBS containing 1% BSA for 30 min and bound rabbit IgG was detected with 15 nm protein A-gold. After fixation with 1.5% glutaraldehyde and negative staining with 3% uranyl acetate, grids were viewed with a Philips CM-10 transmission electron microscope at 100 kV. For ultrastructural analysis of native DMVs, EAV-infected BHK-21 cells grown on coverslips (Thermanox) were cryofixed by high-speed plunge freezing in liquid ethane, freeze substitution, and embedding in LX-112 epoxy resin [30]. Ultrathin sections were contrasted with uranyl acetate and lead hydroxide and viewed with a Philips CM-10 transmission electron microscope at 100 kV.

RESULTS

EAV RTC activity in cytoplasmic extracts.

To study the EAV RTC, we sought to isolate the virus-specific RNA-synthesizing activity from infected BHK-21 cells by mechanical disruption and cell fractionation. Metabolic labeling of EAV RNA synthesis with [³H]uridine revealed that it was maximal by 6 h p.i. (data not shown) and therefore RTCs were routinely isolated at this time point. In general, approximately 10⁸ infected cells were used to prepare a cytoplasmic extract (PNS) with a total protein concentration of 2 to 5 mg/ml.

The PNS described above was used in IVRAs (see Materials & Methods), in which the incorporation of [α -³²P]CTP into viral RNA was analyzed in a reaction mixture containing nucleoside triphosphates (NTPs), Mg²⁺, an energy regenerating system (creatine phosphate and creatine phosphokinase), and an inhibitor of cellular transcription (ActD). We used labeled CTP in our assays to minimize background incorporation that could result from the presence of cellular terminal transferases, which preferentially use ATP and UTP [227].

In a time course experiment (Fig. 1A), we observed the accumulation of several *in vitro*-synthesized, ³²P-labeled RNA species with sizes corresponding to those of the EAV genome (RNA1) and all six sg mRNAs (RNAs 2 to 7). Upon incubations longer than 100 min, the amount of labeled RNA decreased, probably due to the combination of the (continuous) activity of endogenous RNases and a decreasing synthesis rate. The half-life of viral RNA in PNS at 30°C was estimated to be approximately 20 or 40 min, depending on whether we analyzed the integrity of 3'-terminal sequences (hybridization) or the degradation of [³H]uridine labeled RNA molecules to fragments smaller than 20 nt (data not shown). Concurrently, it was found that after a 100-min incubation only 2-10% remained of the endogenous EAV RNA or of an *in vitro*-made transcript when it was added to the assay (data not shown). The addition of fresh reaction components (NTPs and energy regenerating system) at 80 or 100 min into the assay did not boost product formation (data not shown), suggesting that the decrease in incorporation was not due to depletion of reaction components or cellular phosphatases [228], but rather to the absence of (re)initiation of RNA synthesis (in our system) or to loss of RTC activity. We favor the latter explanation, since a >75% reduction in activity was observed when the PNS was preincubated, prior to the IVRA, for 1 h at 4°C or 20°C (with or without reaction components), suggesting that the RTC activity is not very stable at these temperatures (data not shown).

IVRAs performed using varying Mg²⁺ concentrations revealed that RTC activity is strongly dependent on Mg²⁺ with a relatively narrow optimum (Fig. 1B). Further optimization in the 2-4 mM range (data not shown) indicated 2.5 mM Mg²⁺ to be optimal, yielding maximal amounts of EAV-specific RNA products and minimal amounts of host

cell-derived background incorporation. Mg^{2+} could not be replaced by Mn^{2+} , which strongly inhibited the RNA-synthesizing activity (Fig. 1B), even in the presence of Mg^{2+} (data not shown). Addition of Mn^{2+} led to the accumulation of many small, labeled products, suggestive of abortive RNA synthesis, possibly due to compromised RdRp processivity.

IVRAs performed at 25°C, 30°C, and 37°C were compared, with maximum yields obtained at 30°C (data not shown). The optimal pH for the RNA-synthesizing activity was 7.5 (Fig. 1C), since at lower pH hardly any incorporation was observed while at higher pH a decrease in EAV-specific incorporation was accompanied by a strong increase in the synthesis of background products (Fig. 1C). Both the energy regenerating system and exogenous NTPs were essential for activity (Fig. 1D).

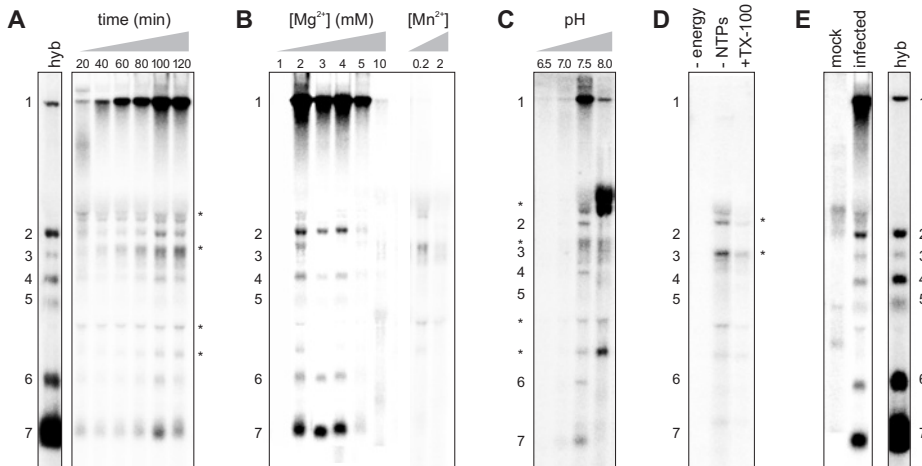


Fig. 1. Reaction products from *in vitro* RNA synthesis assays on cytoplasmic extracts from EAV- and mock-infected cells. Incorporation of $[\alpha\text{-}^{32}\text{P}]\text{CTP}$ in IVRA products was analysed on denaturing formaldehyde-agarose gels followed by PhosphorImager analysis. Marker lanes (hyb) depict the positions of EAV RNA1-7 and contain RNA isolated from infected cells, hybridised with a probe complementary to the 3'-end of all EAV RNAs. The positions of genomic RNA (1) and sg RNA (2-7) are indicated next to the gels. Optimization of reaction conditions. (A) Time course analysis of the RNA synthesis assay. After initiation of an assay, samples were taken at the times indicated above each lane and RNA was isolated and analyzed as described under "Experimental Procedures". (B) IVRAs carried out with varying Mg^{2+} concentrations or in the presence of Mn^{2+} , as indicated above the lanes. (C) Reactions performed at the pH indicated above each lane. (D) Effect of the absence of the energy regenerating system (-energy) or nucleoside triphosphates (-NTP) or the presence of 0.1% Triton X-100 (+TX-100). (E) IVRA performed under fully optimised conditions with cytoplasmic extracts from mock-infected (mock) or EAV-infected cells (infected). * indicates bands that are not EAV-specific and are also detected in assays performed on lysates of mock-infected cells.

Effect of low molecular weight compounds on EAV RTC activity *in vitro*.

Addition of KCl, which stimulated the *in vitro* activity of another RdRp [229], did not increase EAV RTC activity. As reported for other viruses [227, 229], Ca^{2+} strongly inhibited *in vitro* RTC activity, but addition of EGTA had no (stimulating) effect in the case of EAV (data not shown). Ionic and non-ionic detergents like SDS, DOC, NP-40, CHAPS (data not shown) and Triton-X-100 (Fig. 1D) all completely abolished the accumulation of radiolabeled viral RNA when added to IVRAs at 0.5x or 5x their critical micelle concentration, suggesting a crucial role for membranes. Addition of 0.4 mM cap analogue (m7GpppG) had no effect (data not shown), whereas raising the DTT concentration to 10 mM or adding 2 mM spermidine resulted in a 60% and 40% reduction, respectively. Therefore, none of the aforementioned compounds, which have been used to stimulate the *in vitro* activity of replication complexes of other RNA viruses, were included in the assay that was used for further studies.

The translation inhibitor cycloheximide had no significant effect on the *in vitro* RTC activity (data not shown). In conjunction with the observed lack of ^{35}S -methionine incorporation during IVRAs (data not shown), this suggests that (continued) protein synthesis is not required for RdRp activity of the EAV RTC *in vitro*.

Kinetics of EAV RTC activity *in vitro*.

The K_m for NTPs reported for *in vitro* assays with the replication complexes of other RNA viruses is in the range of 3-15 μM [229, 230]. Consequently, we presumed that the low CTP concentration (0.12 μM) would strongly limit RdRp activity when only radiolabeled CTP would be present in EAV IVRAs. To study the kinetics of RNA synthesis by the EAV RTC *in vitro*, reactions were performed with varying amounts of unlabeled CTP (up to 200 μM), using a fixed concentration of 0.12 μM [α - ^{32}P]CTP as a tracer. The incorporation

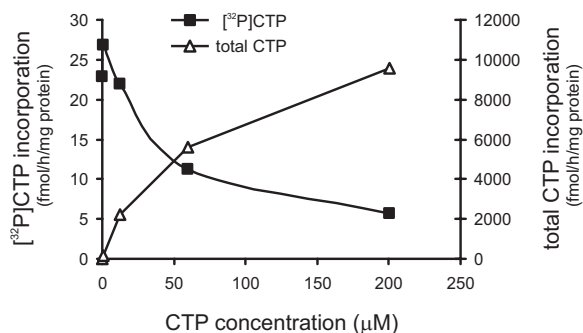


Fig. 2. Kinetics of *in vitro* CTP incorporation into viral RNA by the EAV RTC. The incorporation of [α - ^{32}P]CTP into total viral RNA at various CTP concentrations was quantified as described under "Experimental Procedures" and is expressed as fmol [α - ^{32}P]CTP incorporated per mg of protein per hour reaction time (squares). The total CTP incorporation (triangles) was calculated based on the specific activity of the isotope.

of [α - 32 P]CTP into viral RNA was quantified and the total CTP incorporation was calculated based on the known specific activity (Fig. 2A). At high specific activity, when the [α - 32 P]CTP was not supplemented with cold CTP, ~ 22.4 fmol of [α - 32 P]CTP per mg protein per hour was incorporated into viral RNA (Fig. 2A). At low specific activity, when radiolabeled CTP was supplemented with 200 μ M of unlabeled CTP, the CTP incorporation rate increased over 400-fold to 9,566 fmol/h/mg protein, while the incorporation rate of [α - 32 P]CTP decreased only 4-fold to 5.8 fmol/h/mg protein. For Sindbis virus and West Nile virus similar results have been reported: product detection was better using high specific activity radiolabel, while total CTP incorporation was higher when low specific activities of radiolabel were used [227, 228]. Using a double reciprocal plot of $1/S$ versus $1/V$, the K_m of the RTC for CTP was estimated to be 48 μ M and a V_{max} of 11,000 fmol CTP/h/mg protein was calculated. Using 0.12 μ M [α - 32 P]CTP as a tracer, maximum incorporation of radiolabel was detected when the labeled CTP was supplemented with 0.6 μ M of cold CTP (Fig. 2A). Despite the reaction rate of only 160 fmol CTP/h/mg protein, these conditions were used in subsequent experiments to ensure optimal detection of RNA products.

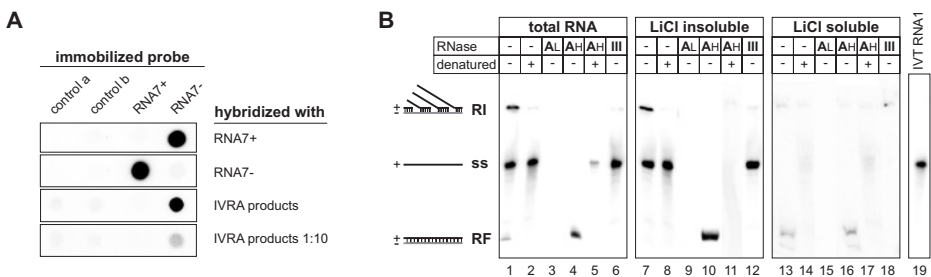


Fig. 3. Analysis of IVRA reaction products. (A) Determination of the polarity of *in vitro* synthesized EAV RNA. Control RNA from L-cells (control a) and Sindbis virus (control b) and RNA probes with either the sense sequence of the 3'-end of the EAV genome (RNA7+) or its complementary sequence (RNA7-) were immobilized on membranes. These membranes were hybridized with 32 P-labeled RNA7+ or RNA7- to determine the specificity of the method and with IVRA reaction products to determine the polarity of *in vitro* synthesized EAV RNA (IVRA products). Hybridization of a membrane with a 1:10 dilution of IVRA products was done to assess the sensitivity of the method. (B) Incorporation of [α - 32 P]CTP into the RI, RF and ss RNA forms of *in vitro* synthesized EAV genomic RNA. After a standard IVRA, isolated total RNA (lanes 1-6) underwent various treatments and was analyzed in a semi-denaturing 7 M urea-3% polyacrylamide gel. Completely double-stranded, LiCl-soluble RF RNA (lanes 13-18) was separated from LiCl-insoluble ss and partially ss RI RNAs (lanes 7-12) by fractionation in 2 M LiCl. Samples were treated with RNaseA/T1 either using high salt conditions (AH), under which ss RNA is specifically degraded, or under low salt conditions (AL), causing degradation of all RNA. Double-stranded RNA was specifically degraded by RNase III treatment, as indicated above the lanes (III). Some samples were heat-denatured prior to running the gel. The position of ss RNA1 in this gel system was determined using 32 P-labeled *in vitro* transcribed RNA1 (IVT RNA1). Only RNA1 is visible in this figure, as the sg RNAs migrated off the gel under the electrophoresis conditions applied. The positions of RI, RF and ss RNA are indicated next to the gel.

EAV RTC activity *in vitro* under optimized conditions.

Fig. 1E depicts the results of a fully optimized IVRA performed using PNS from mock- and EAV-infected cells. Besides EAV-specific products, several minor labeled RNA species with sizes not corresponding to those of the known EAV RNAs were observed. Probably these are cellular RNAs since they were also, often more prominently, detected in assays performed with PNS from mock-infected cells (Fig. 1E). Since host cell nuclei had been removed and ActD was present, it is unlikely that these aberrant products resulted from (residual) host cell transcription. Hence, cellular activities, such as terminal transferases, were likely responsible for the labeling of host RNAs [227]. A severe reduction in the synthesis of EAV-specific radiolabeled RNA products was observed when using CTP as the only NTP in the reaction (Fig. 1D), indicating that a bona fide RdRp activity rather than a template- and NTP-independent terminal transferase activity was monitored in our assay. The intensity of the background bands could be minimized by carefully optimizing the reaction conditions (especially with respect to pH and Mg^{2+} concentration), resulting in the majority of label being incorporated into EAV-specific products.

Characterization of EAV-specific RNAs synthesized *in vitro* by the RTC.

To determine the polarity of the EAV RNAs that are produced by the EAV RTC *in vitro*, ^{32}P -labeled IVRA products were hybridized to membranes containing immobilized sense (RNA7+) or antisense (RNA7-) probes representing a part (ORF7) of the 3'-proximal region of the EAV genome (Fig. 3A). The specificity of this method was confirmed by hybridizing these membranes with ^{32}P -labeled, *in vitro* produced RNA7+ and RNA7- control transcripts (Fig. 3A). The ^{32}P -labeled IVRA products strongly hybridized to the RNA7- probe (Fig. 3A), indicating that the EAV RNAs synthesized were mainly of positive polarity. The quantity of radiolabeled material that hybridized to immobilized RNA7+ or control RNA was at least 60-fold less than that captured by the RNA7- probe. The fact that negative sense products were hardly detected was not due to low sensitivity of the assay, as the positive sense RNA was still readily detectable when 10x less IVRA products were used in the hybridization assay (Fig. 3A).

To study the incorporation of $[\alpha\text{-}^{32}P]\text{CTP}$ into RI, RF and ss RNAs, reaction products were analyzed by LiCl fractionation and by treatment with RNases that specifically degrade either ds or ss RNA. Subsequently, products were analyzed in a semi-denaturing 7 M urea-3% polyacrylamide gel (Fig. 3B), allowing the separation of the RI, RF and ss RNA forms [226]. In view of the anticipated complexity of the data for the various sg RNAs (which would yield a complex pattern of up to 18 additional bands), the present analysis is limited to genomic RNA and the analysis of the RI, RF and ss forms of the sg RNAs will be described elsewhere.

Approximately 68% of the radiolabel was detected in a product that migrated at the position of ss RNA1, 30% was in a slower migrating RI and 2% of the label was found

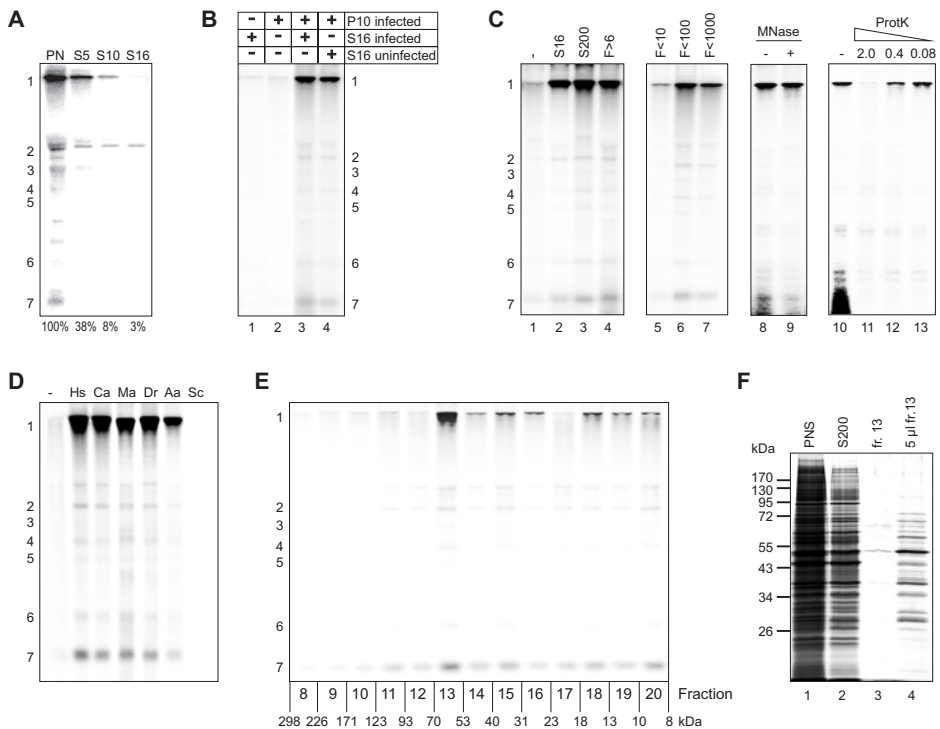


Fig. 4. Characterization of a host factor required for EAV RTC activity. IVRAs were performed and products were analyzed as described in the legend to Fig. 1. (A) RTC activity in cellular fractions obtained by differential centrifugation of the PNS. IVRAs were performed on the lysate before centrifugation (PNS) and the supernatant after centrifugation for 10 minutes at 5,000 x g (S5), 10,000 x g (S10) and 16,000 x g (S16). (B) IVRAs containing either S16 or P10 alone or P10 supplemented with either S16 from infected cells or mock-infected cells as indicated above the lanes. (C) Ability of fractions to stimulate activity of sedimented RTCs. IVRAs were performed with 5 μ l P10 supplemented with 20 μ l of dilution buffer (lane 1) or various fractions (lanes 2-13). S16 & S200, 16,000 x g and 200,000 x g supernatant fractions prepared from the PNS of EAV-infected cells. F>6 was prepared from S16 by removal of molecules with a molecular mass <6 kDa by size exclusion chromatography. F<10, F<100 and F<1000 were prepared from S16 by ultrafiltration over filters with 10, 100 and 1000 kDa cut-offs, respectively. S16 was treated (+) or mock-treated (-) with micrococcal nuclease (MNase) or 0, 2.0, 0.4 or 0.08 mg/ml proteinase K as indicated above lanes 10-13. (D) IVRAs performed with RTCs isolated from infected BHK-21 cells (5 μ l of P10) and supplemented with 20 μ l of dilution buffer (-) or 20 μ l of S200 fractions from HeLa cells (*Homo sapiens*; Hs), Vero E6 cells (*Cercopithecus aethiops*; Ca), BHK-21 cells (*Mesocricetus auratus*; Ma), 1-day old zebrafish embryos (*Danio rerio*; Dr), C6/36 cells (*Aedes albopictus*; Aa) or yeast cells (*Saccharomyces cerevisiae*; Sc), all diluted to result in the addition of 30 μ g of total protein per IVRA reaction. (E) Purification of the host factor from a HeLa cell S200 fraction by gel filtration. IVRAs were performed with isolated RTCs (P10) supplemented with various fractions from the gel filtration column, as indicated at the bottom of the gel. The molecular mass range of each fraction was extrapolated from a calibration curve and is indicated under the fraction numbers. (F) Analysis of 0.5 μ l of PNS, S200, and column fraction 13 by SDS-PAGE and silver staining (lane 1-3). Lane 4 contains 5 μ l of column fraction 13.

in the faster migrating RF form of RNA1 (Fig. 3B, lane 1). When the IVRA products were heat-denatured prior to electrophoresis, a product migrating at the position of ss RNA was visible (Fig. 3B, lane 2). After degradation of ss RNA by RNase A/T1 treatment under high salt conditions, only a band at the position of the nuclease resistant RF form was observed (Fig. 3B, lane 4). The increased intensity of the RF band in lane 4 (compared to lane 1) was likely due to the redistribution of label from the RI form, which was converted into RF through degradation of nascent strands. Likewise, the denaturation of RNase A/T1-treated RNA converted the RF into ssRNA (lane 5). All RNAs were completely degraded upon RNase A/T1 treatment under low salt conditions (lane 3). After treatment with the ds RNA-specific RNase III, labeled products were observed almost exclusively at the position of ss RNA1 (lane 6).

The LiCl-insoluble fraction contained the (partially ss) RI and ss RNA1 and no RF RNA, the latter being LiCl-soluble (Fig. 3B, lane 7 and 13). After RNase A/T1 treatment of the LiCl pellet fraction, the ss RNA was no longer detectable and the RI was converted into the RF (Fig. 3B, lane 10). Upon denaturation of this sample, the band migrating at the RF position disappeared and a smear appeared at the position between the ssRNA and RF bands in the gel, which probably represented abrogated and partially degraded labeled molecules that had originally been part of the ds regions of the RI (lane 11).

The RF form was soluble in 2 M LiCl (Fig. 3B, lane 13), which indicates that it was completely double-stranded. This was further substantiated by the observation that it was fully degraded by RNase III and completely resistant to RNase A/T1-treatment (lanes 16 and 18). After denaturation of LiCl-soluble RNA that was either untreated or RNase A/T1-treated, a discrete band migrating at the expected position of ssRNA was observed. This indicates that, unlike the RI (lane 11), the RF was completely double-stranded and consisted of two full-length molecules of opposite polarity (lanes 14 and 17).

Taken together, these data indicate that the EAV RTC catalyzed the incorporation of nucleotides into the RI and RF forms of RNA1 *in vitro* and that ss genomic RNA was released from (one or both of) these forms.

EAV RTC activity depends on a cytosolic host factor.

To determine whether isolation of active EAV RTCs can be achieved by differential centrifugation, we first determined the g-force required to remove RdRp activity from the PNS. Supernatants prepared by centrifugation at 5,000 x g, 10,000 x g, or 16,000 x g retained 38%, 8%, and 3% of the activity, respectively (Fig. 4A). For subsequent experiments pelleting at 10,000 x g was used, as we were able to routinely remove about 95% of activity from the PNS, while the pellet could still be readily resuspended (this was more difficult for a 15,000 x g pellet, increasing the risk of mechanical damage to the RTC by sheering forces). The activity producing the background product migrating directly above RNA2 in all lanes of the gel in Fig. 4A remained in the cytosolic fractions,

suggesting that it is soluble, and could thus be separated from the RTC by this method. Surprisingly, the resuspended P10 pellet only exhibited very weak RTC activity (Fig 4B, lane 2). However, this activity could be stimulated considerably with an aliquot of a supernatant fraction (S16; lane 3). Importantly, S16 prepared from mock-infected cells was equally capable of restoring the RTC activity of P10, demonstrating that the factor involved must be of host origin (lane 4).

To determine the nature of the host factor required for RTC activity, the S16 fraction was fractionated by centrifugation, ultrafiltration, and size exclusion chromatography, and was also treated with either a nuclease or a protease (Fig. 4C). The host factor did not pellet at 200,000 x g (Fig. 4C, lane 3), suggesting it is a soluble cytosolic component, not

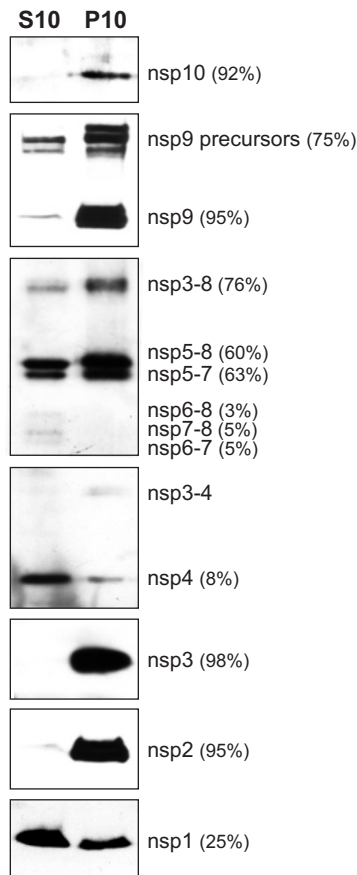


Fig 5. Distribution of nsps after fractionation of the PNS from EAV-infected cells into a 10,000 x g supernatant (S10) and RTC-containing pellet (P10). Equivalent amounts of S10 and P10 derived from the same number of cells were analyzed by Western blotting with anti-nsp10, anti-nsp9, anti-nsp7-8, anti-nsp4, anti-nsp3, anti-nsp2, and anti-nsp1 antibodies. Numbers in brackets indicate the percentage of the protein that is present in the P10 fraction.

associated with cellular organelles. A fraction from which molecules smaller than 6 kDa had been removed by size exclusion chromatography retained the ability to activate the isolated RTC (Fig. 4C, lane 4), indicating that the factor(s) is not a low molecular weight compound, like an NTP or metal ion. The host factor was removed by ultrafiltration using a filter with a 10 kDa cut-off value, but passed through filters with 100 kDa or 1000 kDa cut-offs (Fig. 4C, lanes 5-7). Nuclease treatment had no effect, while protease treatment destroyed the ability of an S16 fraction to activate pelleted RTCs (Fig. 4C, lanes 8-13). Taken together these data indicate that the host factor that is required for the activity of isolated RTCs is a soluble cytosolic protein with a native molecular mass in the range of 10-100 kDa.

To determine whether the host factor is also present in other cell types than BHK-21 cells, S200 fractions from various (uninfected) mammalian, fish, insect and yeast cells were tested for their ability to activate RTCs isolated from EAV-infected BHK-21 cells (Fig. 4D). With the exception of yeast, S200 fractions from all organisms tested were able to reconstitute RTC activity of the P10 fraction, indicating that the host factor is likely to be conserved in animal cells.

The host factor was further purified from a HeLa cell S200 fraction by gel filtration chromatography, since we anticipated that the available data on the human genome and proteome would facilitate future identification of the factor by e.g. mass spectrometry. Each gel filtration fraction was analyzed for the presence of the host factor by adding it to an IVRA with pelleted RTCs (P10 fraction) isolated from EAV-infected BHK-21 cells (Fig. 4E). Fraction 13, which contains proteins with a mass of 53-70 kDa, exhibited the maximum stimulatory effect on RTC activity (Fig. 4E). In an independent experiment, in which slightly different column fractions were collected, the host factor was retrieved in the fraction containing 59-78 kDa proteins (data not shown). Taken together these studies suggest that the (native) mass of the host factor is between 59 and 70 kDa.

Compared to PNS or an S200 fraction, the protein concentration of column fraction 13 was greatly reduced and its composition was clearly less complex (Fig. 4F, lane 1-3), without affecting its ability to stimulate the RTC, indicating that we have achieved a significant purification of the host factor. However, fraction 13 still contained over 30 proteins, as could be observed when a 10-fold larger sample was analyzed (Fig. 4F, lane 4), and therefore additional purification steps will be required for the unequivocal identification of the host factor. A potential complicating factor for this follow-up might be that the host factor is (part of) one of the homo- or hetero-multimeric complexes that are apparently present in fraction 13, which would explain the presence of several polypeptides with a mass smaller than 53 kDa in this fraction (Fig. 4F, lane 4).

Quantitative analysis revealed that the sedimentation procedure used to prepare P10 fractions led also to a substantial non-recoverable loss of RTC activity with a significant variation between individual experiments. Typically, 10-50% of the activity that was

originally present in the PNS could be recovered in P10 fractions when assayed in the presence of the trans-activating host factor. The considerable loss of activity was apparently not due to the resuspension procedure of the RTC pellets, since resuspending less vigorously or not at all further reduced the recovery of activity (data not shown). The P10 fractions typically contained 3-7% of the protein that was present in the PNS. Therefore, despite the low yield, a 2- to 13-fold increase in specific RTC activity was achieved when comparing P10- to PNS-based samples.

Distribution of EAV nsps between S10 and P10 fractions.

To start defining the composition of the RTC and the potential roles of the various EAV nsps in viral RNA synthesis, the distribution of these proteins between the P10 and S10 fractions was investigated by western blotting (Fig. 5). As anticipated, nsp2 and nsp3 were almost exclusively present in the P10 fraction. These subunits contain hydrophobic domains [33, 202], have been implicated in virus-induced membrane modifications, and likely are a structural component of the DMVs [217]. The nsp9-RdRp and nsp10-helicase subunits were also predominantly found in P10. Significant amounts of larger nsp9 precursors were recovered from the cytosolic S10 fraction, likely representing replicase polyproteins and cleavage intermediates, whose processing is relatively slow [223]. Mature nsp4-main protease largely remained in S10, separated from the nsp9-RdRp and nsp10-helicase, suggesting its presence is not (or no longer) required for RTC activity. On the other hand the long-lived nsp3-4 processing intermediate [231] was present in the P10 fraction, probably through membrane association of its hydrophobic nsp3 part [33]. Also a large proportion of the nsp3-8, nsp5-8 and nsp5-7 intermediates cosedimented with the RTC, probably as a result of the membrane-association of the hydrophobic nsp5 part of these proteins. Polypeptides lacking this hydrophobic domain, like the nsp6-8,

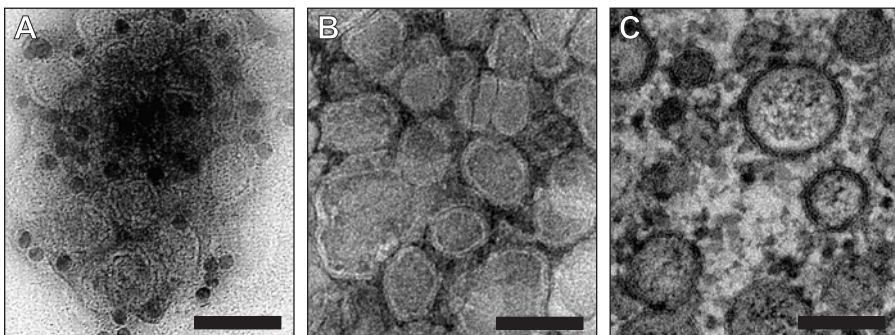


Fig 6. Electron micrographs of the RTC-containing P10 fraction and EAV-infected cells. (A) Immunoelectron microscopy with anti-nsp3 rabbit serum on the chemically fixed P10 fraction. (B) Control labeling of the P10 fraction with preimmune serum from the same animal. (C) Electron micrograph of a thin section of cryofixed EAV- infected BHK-21 cells. Scale bar: 100 nm.

nsp7-8 and nsp6-7 products of the minor proteolytic processing pathway [232], were mainly recovered from the cytosolic fraction (Fig. 5). In the case of nsp1, a multifunctional autoprotease whose zinc finger domain has been directly implicated in EAV transcription [233-235], approximately 75% of the protein was found in the cytosolic S10 fraction, but ~25% of the protein was recovered from the RTC-containing P10 fraction, which is in line with its essential role in sg RNA synthesis. A comparable nsp1 distribution was observed *in vivo* by immunofluorescence microscopy of infected cells (D.D. Nedialkova, E.J. Snijder, *et al.*, unpublished observations).

DMVs are present in the RTC-containing P10 fraction.

The RTC-containing P10 fraction was analyzed by electron microscopy (negative staining) in combination with an immunogold labeling for nsp3 (Fig. 6A). The fraction contained abundant vesicles with a diameter of 60-80 nm that clearly appeared to have a double membrane and labeled strongly when using an anti-nsp3 rabbit serum. Immunogold labeling was not observed when the preimmune serum of the same rabbit

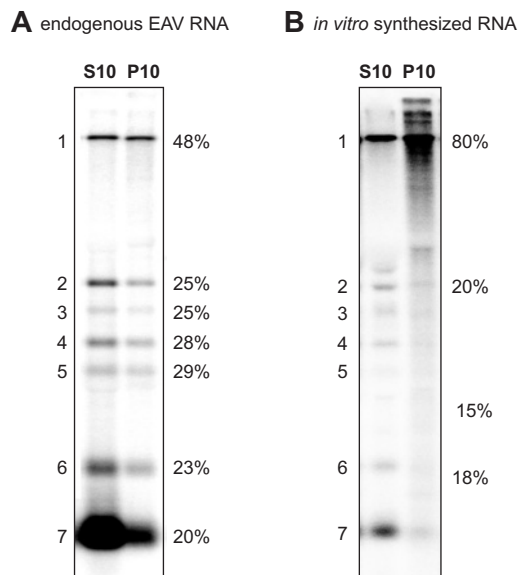


Fig 7. Distribution of endogenous and newly *in vitro* synthesized EAV RNA. (A) Distribution of endogenous EAV RNA. Viral RNA recovered from the 10,000 x g supernatant (S10) and pellet (P10) obtained after centrifugation of the PNS of EAV-infected cells was analyzed by denaturing formaldehyde-agarose electrophoresis and hybridization with a ³²P-labeled probe complementary to the 3'-end of all EAV RNAs. (B) Distribution of *in vitro* synthesized EAV RNA. After an IVRA, the PNS was fractionated into a 10,000 x g supernatant (S10) and pellet (P10). ³²P-labeled *in vitro* synthesized RNA was visualized by denaturing formaldehyde-agarose electrophoresis and direct PhosphorImager analysis. The percentage of each RNA species that is present in the P10 fraction is indicated to the right of each gel. Numbers for RNA 3, 4, 5 are absent in panel B because the signal obtained with the P10 fraction was too low to be reliably quantified.

was used (Fig. 6B). These structures were slightly smaller than the DMVs observed in infected cells (Fig. 6C; [201]), which might be due to differences in fixation methods. The overall morphology, presence of a double membrane, and abundant presence of nsp3 were all consistent with the notion that the P10 fraction is enriched for the virus-induced DMVs that are observed in EAV-infected cells. Such structures were not observed in P10 fractions prepared from mock-infected cells (data not shown).

Distribution of EAV RNA between S10 and P10 fractions.

The distribution of endogenous EAV RNA between the P10 and S10 fractions was analyzed by quantitative hybridization of RNA isolated from these fractions using a probe complementary to the 3'-end of all EAV mRNAs. Endogenous genomic RNA was approximately evenly distributed between the cytosolic S10 fraction and the RTC-containing P10 (Fig. 7A). Conversely, sg mRNAs were mainly recovered from the cytosolic S10 fraction (Fig. 7A). This differential distribution of genome versus sg mRNA was even more striking for newly synthesized RNA that was labeled *in vitro* using PNS, after which a fractionation into P10 and S10 was performed (Fig. 7B). The bulk of newly made genomic RNA remained associated with the RTC in P10, while only a small fraction, presumably single-stranded RNA released from the RTC, was present in S10. In contrast, newly made sg mRNAs were mainly recovered from the cytoplasmic S10 fraction suggesting their rapid release from the complex in which they had been synthesized.

DISCUSSION

Characterization of EAV RTC activity *in vitro*.

In this study, we describe the first procedure for the isolation of an active arterivirus RTC from infected cells and the initial biochemical characterization of its composition and RNA synthesizing activity. Using EAV, one of the best studied nidovirus models, we succeeded in obtaining an RTC preparation capable of the *in vitro* synthesis of both viral genomic RNA and all sg RNAs. The isolated RTC incorporated radiolabel into EAV-specific products in a reaction mixture containing [α - 32 P]CTP, Mg $^{2+}$ and an energy regenerating system. The absence of such products in IVRAs performed with lysates from mock-infected cells, and their dependence on the presence of all four NTPs, demonstrated that they resulted from genuine viral RdRp activity. To our knowledge, this is the first robust *in vitro* system for nidovirus replication and transcription. RdRp activity in cell lysates has been reported previously for the (very distantly) related coronaviruses MHV and TGEV [236-240], but these activities were in some cases barely detectable and appeared to be rather unstable. Furthermore, reaction products were not characterized [236, 238], there were discrepancies between the sizes of *in vitro* and *in vivo* synthesized viral RNA

[237, 240], only genome-sized RNA was detected [239] or conflicting observations were reported [237-239, 241]. The EAV *in vitro* assay described here should facilitate studies into the role of membranes, host factors and viral proteins involved in replication and transcription and allow for the more detailed characterization of the nidovirus RTC at the molecular level.

Up to 100 min into the reaction, radiolabeled products accumulated, after which a decrease was observed, probably due to a decreasing RNA synthesis rate in combination with a steady rate of degradation by cellular nuclease activity. Consistent with our results, nucleases in BHK-21 cell extracts were previously reported to be responsible for the cessation of *in vitro* RdRp activity of other viruses [228, 242, 243]. The K_m for CTP of the EAV RTC was estimated to be 48 μM , slightly higher than values (3-15 μM) reported for other viruses [229, 230] and the V_{max} of CTP incorporation was calculated to be approximately 11,000 fmol/h/mg protein. This is approximately 5-fold higher than the *in vitro* RdRp activity reported for several flaviviruses (1000-2700 fmol/h/mg; [229, 244, 245]), more than 20-fold higher than activities previously reported for brome mosaic virus (59) and the coronaviruses TGEV [240] and MHV [236], and 5- to 20-fold lower than values reported for several alpha- and picornaviruses [228, 246-248]. For EAV an up to 13-fold increase in specific activity could be achieved when the RTC was partially purified by sedimentation at 10,000 x g. Incorporation of radiolabel into the RI, RF and ss forms of EAV RNA1 was observed, mainly into RNA of positive polarity, which is in line with the asymmetric synthesis of a large excess of plus strands over minus strands that is commonly observed *in vivo*.

The *in vitro* activity of the EAV RTC was strongly dependent on Mg^{2+} , as also reported for other positive-stranded RNA viruses [227, 229, 230, 236, 239, 244, 246-258]. For EAV, Mn^{2+} could not replace Mg^{2+} , and had a strong inhibitory effect, even at low concentrations and despite the presence of Mg^{2+} . This suggested that it competes for Mg^{2+} binding, while interfering with enzymatic activity. EAV RTC activity was also inhibited by other divalent cations, like Zn^{2+} and Ca^{2+} (manuscript in preparation), as has also been found for West Nile virus and Japanese encephalitis virus RdRp activity [227, 229]. A strong inhibitory effect of Mn^{2+} on *in vitro* RdRp activity was reported for various other viruses [240, 246, 247, 250, 252, 259], although for several flaviviruses Mn^{2+} could substitute for Mg^{2+} to a limited extent [227, 229, 253-255, 257, 260]. Addition of Mn^{2+} to the EAV IVRA promoted the accumulation of small products, suggesting elongation/processivity was affected, as was observed for Japanese encephalitis virus, hepatitis C virus and brome mosaic virus [229, 255, 261]. The inhibition of the EAV RTC activity by Mn^{2+} contrasts with the Mn^{2+} -dependence of the purified EAV nsp9-RdRp that was recently reported [215]. However, this nsp9-RdRp activity was only observed on artificial templates rather than natural templates.

An energy regenerating system was essential for EAV RTC activity, which might for example be due to the ATP-dependence of the nsp10-helicase that presumably plays a key role in RNA synthesis and/or release of ss RNA. Supporting this idea, in a pestivirus *in vitro* RdRp assay, radiolabel was only detected in ds RNA and no longer in ss RNA in the absence of an energy regenerating system [245].

Thus far, it remains unclear whether the isolated RTC is capable of initiation of viral RNA synthesis *in vitro* or is only elongating nascent RNA molecules (plus strands in RIs) initiated *in vivo*. Continuous incorporation of label in short sg RNAs, like RNA7, up to 100 min after the start of the assay might indicate initiation of RNA synthesis *in vitro*, since in the absence of initiation, accumulation of short RNAs would be expected to peak before that of longer molecules. On the other hand, the isolated RTC did not evidently utilize an exogenous replication-competent plus strand RNA (replicon EDI [262]) as template for RNA synthesis (data not shown). However, it should be noted that such a positive sense RNA may be a poor template in our assay for a variety of reasons related to the properties of the RTC, like the predominant synthesis of plus strands, exogenous macromolecules being unable to enter (preformed) membrane-associated RTCs, or RTC formation occurring in *cis*, e.g. in conjunction with translation of the RNA, which is not likely to occur in this *in vitro* assay (see below). In support of this latter notion, it was found that preformed poliovirus replication vesicles, resulting from the expression of viral proteins, did not participate in the formation of active replication complexes after poliovirus superinfection [263].

No measurable protein synthesis was observed in our PNS and the addition of the translation inhibitor cycloheximide had little effect on viral RNA synthesis *in vitro*, suggesting that continued protein synthesis is not required for *in vitro* RTC activity, as was also reported for poliovirus, hepatitis C virus and Kunjin virus [264-266]. However, for the coronavirus MHV, translation inhibition blocked viral RNA synthesis (particularly minus strand synthesis) both *in vivo* [241] and *in vitro* [236, 239]. These conflicting observations, might reflect fundamental differences in the mechanism of replication of arteri- and coronaviruses or might be due to technical differences between the systems used.

The activity of isolated RTCs depends on a cytosolic host factor.

EAV RTC activity was associated with heavy membrane structures that could be sedimented from PNS at 10,000 x g (P10). The addition of non-ionic detergents destroyed all RTC activity, consistent with an important role of membranes in RTC structure and/or function, a common feature of many positive-stranded RNA viruses. Hardly any RTC activity was detected in the resuspended P10 fraction when it was assayed in a standard IVRA. The activity was however considerably stimulated when the reaction was supplemented with the S16 fraction from either infected or mock-infected BHK-21 cells, and

further experiments suggested that a cytosolic host protein is required for RTC activity. This host factor was also present in the cytosol of the various mammalian, fish and insect cells that were tested, but not in yeast cells, suggesting it is highly conserved in animal cells (Fig. 4D). The host factor was partially purified from the cytosol of HeLa cells by gel filtration chromatography, revealing a native mass of between 59 and 70 kDa. The future, unambiguous identification of the host protein factor required for EAV RTC activity will depend on the successful development of a protocol allowing its further purification without loss of activity. Follow-up studies to explore this issue are currently in progress.

Besides EAV, the fact that the activity of isolated membrane-associated viral replication complexes depends on a host factor has only been reported for poliovirus [264] and not for the isolated membrane-associated replication complexes of various other viruses [229, 255, 267-270]. Whether this is due to fundamental differences between replication complexes of different viruses or due to variations in isolation and assay procedures remains to be seen. For instance, host factors might be involved in the RNA synthesis of all viruses, but their copurification with the active complex might depend on the mode of their association with the replication complex.

Structural characterization of the isolated EAV RTC.

Ultrastructural analysis of the RTC-containing heavy membrane pellet fraction by immunoelectron microscopy revealed the presence of nsp3-containing DMVs, resembling those observed in EAV-infected cells [201]. Analysis of the distribution of replicase subunits between the cytoplasmic S10 fraction and the RTC-containing P10 fraction, revealed that proteins previously implicated in viral RNA synthesis (nsp9-RdRp and nsp10-helicase; [215, 216]) and DMV formation (nsp2 and nsp3; [217]) exclusively cosedimented with the active RTC. In contrast, the main protease nsp4 was found predominantly in the cytosolic S10 fraction and not cosedimenting with RTC activity, suggesting its presence is not (or, rather, no longer) required for RTC activity. The P10 fraction also contained substantial amounts of the nsp3-8, nsp5-8, nsp5-7 processing intermediates and the multifunctional nsp1 [233-235], which is in line with its essential role in sg RNA synthesis. In general, these data are in agreement with previously reported immunofluorescence and electron microscopy data [33, 201, 202].

The bulk of newly synthesized EAV genomic RNA remained associated with the RTC, while sg mRNAs were mainly found in the cytoplasmic fraction, suggesting their rapid release from the complex by which they had been synthesized. It is unlikely that the relative enrichment in genomic RNA is merely due to the slow release of labelled ss RNA from the RI, as 68% of radiolabel was present in the ss form and only 30% in the RI form of RNA1. These results might reflect the existence of separate pools of RNAs with distinct roles in the viral life cycle. The molecules that were released from the RTC might be destined for translation, leading to the synthesis of structural proteins (mRNA2-7)

and additional replicase subunits (mRNA1). The RNA1 molecules that remained associated with the RTC might serve as new templates for replication and transcription and/or become incorporated into new virions, assuming packaging occurs in coordination with replication. In this context, the reported partial colocalization of the N protein with the RTC of EAV [270] and other nidoviruses [32] is an interesting observation. Intracellular virions that were already present upon cell lysis probably contributed to the amount of (mainly unlabeled) endogenous genomic RNA recovered from the cytosolic fraction.

In conclusion, DMV-like double membrane structures, newly *in vitro* synthesized viral RNA, and several key replicase subunits cosedimented with EAV RTC activity, which was also found to be dependent on a cytosolic host factor. Taken together, these data confirm and extend the link between these modified membranes and nidovirus replication and transcription. Our analysis indicates that membranes are essential for RTC function, e.g. to protect the RTC against the observed cellular nuclease activity. In addition, sequestering the RTC in specific membrane-bounded compartments might be important for separating and/or coordinating different processes in the viral life-cycle (e.g. replicase processing, replication, translation, and packaging), which might be reflected by the differential distribution of genomic and sg RNA and the various viral proteins.

ACKNOWLEDGMENTS

We thank Kèvin Knoops and Mieke Mommaas from the Section Electron Microscopy, Department of Molecular Cell Biology, Leiden University Medical Center for electron microscopy, Peter Bredenbeek for C6/36 cells, and Danny Nedialkova for sharing materials and interesting discussions. Zebrafish embryos were a generous gift of Christoph Bagowski of the Department of Integrative Zoology, Institute of Biology, Leiden University. This research was supported by a grant from the Council for Chemical Sciences of the Netherlands Organization for Scientific Research (NWO-CW grant 700.52.306).